



Caroline Akemi Hassegawa¹ 

Michele Alves Garcia-Usó² 

Marília Sakayo Yatabe-Ioshida³ 

Inge Elly Kiemle Trindade^{4,5} 

Ana Paula Fukushiro^{4,6} 

Daniela Gamba Garib Carreira^{7,8} 

Ivy Kiemle Trindade-Suedam^{4,5} 

Internal nasal dimensions of children with unilateral cleft lip and palate and maxillary atresia: comparison between acoustic rhinometry technique and cone-beam computed tomography

Dimensões internas nasais de crianças com fissura labiopalatina e deficiência maxilar: comparação entre a técnica de rinometria acústica e a tomografia computadorizada de feixe cônico

Keywords

Cleft Palate

Nasal Cavity

Acoustic Rhinometry

Cone-Beam Computed Tomography

Respiration

Descritores

Fissura Palatina

Cavidade Nasal

Rinometria Acústica

Tomografia Computadorizada de Feixe

Cônico

Respiração

ABSTRACT

Purpose: To compare the nasal cavity geometry of children and teenagers with cleft lip and palate and maxillary atresia by two methods: cone-beam computed tomography, considered the gold standard, and acoustic rhinometry. **Methods:** Data on cone-beam computed tomography and acoustic rhinometry examinations of 17 children and teenagers with cleft lip and palate and maxillary atresia, previously obtained for orthodontic planning purposes, were evaluated prospectively. Using Dolphin Imaging 11.8 software, the nasal cavity was reconstructed by two evaluators, and the internal nasal volumes were obtained. Using rhinometry, the volumes of regions V1 and V2 were measured. The values of each examination were then compared at a significance level of 5%. **Results:** Statistical analysis showed high intra- and inter-rater reproducibility in the cone-beam computed tomography analysis. The mean internal nasal volumes (\pm standard deviation) obtained using acoustic rhinometry and cone-beam computed tomography corresponded to 6.6 ± 1.9 cm³ and 8.1 ± 1.5 cm³, respectively. The difference between the examinations was 17.7%, which was considered statistically significant ($p = 0.006$). **Conclusion:** The nasal volumes measured via the two methods were different; that is, they presented discrepancies in the measurements. The gold standard technique identified larger volumes than acoustic rhinometry in the nasal cavity. Therefore, determining which test reflects clinical reality is an essential future step.

RESUMO

Objetivo: Comparar a geometria da cavidade nasal de crianças e adolescentes com fissura labiopalatina e deficiência maxilar por meio de dois métodos: a tomografia computadorizada de feixe cônico, considerada padrão-ouro, e a rinometria acústica. **Método:** Foram avaliados, de maneira transversal, os exames de tomografia computadorizada de feixe cônico e de rinometria acústica, previamente obtidos para fins de planejamento ortodôntico, de 17 crianças e adolescentes com fissura labiopalatina e atresia maxilar. Por meio do programa *Dolphin Imaging 11.8*, a cavidade nasal das imagens tomográficas foi reconstruída por dois avaliadores e foram obtidos os volumes internos nasais. Por meio da rinometria, os volumes nasais foram aferidos para as regiões V1 e V2. Os valores de cada exame foram, então, comparados, a um nível de significância de 5%. **Resultados:** A análise estatística mostrou alta reprodutibilidade intra e interavaliadores na análise da tomografia computadorizada de feixe cônico. Os volumes internos nasais médios (\pm desvio-padrão), utilizando a rinometria acústica e a tomografia computadorizada de feixe cônico corresponderam a $6,6 \pm 1,9$ cm³ e $8,1 \pm 1,5$ cm³, respectivamente. A diferença entre os exames foi de 17,7%, considerada estatisticamente significante ($p = 0,006$). **Conclusão:** Os volumes nasais aferidos pelos dois métodos são diferentes, ou seja, apresentam discrepâncias nas medidas. A técnica considerada padrão-ouro identificou volumes maiores na cavidade nasal. A determinação de qual exame reflete a realidade clínica constitui passo futuro importante.

Correspondence address:

Ivy Kiemle Trindade-Suedam
Departamento de Ciências Biológicas,
Faculdade de Odontologia de
Bauru, Universidade de São Paulo e
Laboratório de Fisiologia, Hospital
de Reabilitação de Anomalias
Craniofaciais, Universidade de São
Paulo – FOB USP e HRAC USP
Rua Silvio Marchione, 3-20, Vila Nova
Cidade Universitaria, Bauru (SP),
Brasil, CEP: 17012-900.
E-mail: ivytrin@usp.br

Received: April 17, 2020

Accepted: June 24, 2020

Study conducted at Hospital de Reabilitação de Anomalias Craniofaciais, Universidade de São Paulo – HRAC USP – Bauru (SP), Brasil

¹ Programa de Pós-graduação, Laboratório de Fisiologia, Hospital de Reabilitação de Anomalias Craniofaciais, Universidade de São Paulo – HRAC USP - Bauru (SP), Brasil.

² Centro Universitário das Faculdades Integradas de Ourinhos – UNIFIO - Ourinhos (SP), Brasil.

³ Departamento de Ortodontia e Odontopediatria, School of Dentistry, University of Michigan – UM - Ann Arbor (MI), USA.

⁴ Laboratório de Fisiologia, Hospital de Reabilitação de Anomalias Craniofaciais, Universidade de São Paulo – HRAC USP - Bauru (SP), Brasil.

⁵ Departamento de Ciências Biológicas, Faculdade de Odontologia de Bauru, Universidade de São Paulo – FOB USP - Bauru (SP), Brasil.

⁶ Departamento de Fonoaudiologia, Faculdade de Odontologia de Bauru, Universidade de São Paulo – FOB USP - Bauru (SP), Brasil.

⁷ Setor de Ortodontia, Hospital de Reabilitação de Anomalias Craniofaciais, Universidade de São Paulo – HRAC USP - Bauru (SP), Brasil.

⁸ Departamento de Ortodontia, Faculdade de Odontologia de Bauru – FOB USP - Bauru (SP), Brasil.

Financial support: FAPESP (2017/12789-9).

Conflict of interests: nothing to declare.



This is an Open Access article distributed under the terms of the Creative Commons Attribution License, which permits unrestricted use, distribution, and reproduction in any medium, provided the original work is properly cited.

INTRODUCTION

Cleft lip and palate (CLP) are congenital malformations that occur in the face and are formed early in the embryonic period, up to approximately the 12th week of pregnancy, resulting from the absence of fusion of the embryonic facial processes (maxillary, mandibular, nasal, and palatal)^(1,2).

Individuals with CLP undergo several interventions in their rehabilitation process, starting with the primary surgeries of the lip (cheiloplasty) and palate (palatoplasty), which aim to reconstruct the morphological defect early in childhood⁽³⁾. However, CLP also has an impact on nasal shape and function. These changes generally reduce the internal nasal cavity, interfering with air flow, leading to oral breathing, and influencing craniofacial development⁽⁴⁾. Bearing this in mind, the treatment of individuals with CLP also involves surgeries to correct the septum, base, nasal bone, and other structures of the nose⁽⁵⁾, the so-called secondary surgeries.

Specifically, regarding the nasal cavity, a study demonstrated that children with complete unilateral and bilateral CLP have reduced internal nasal dimensions, in the order of 30% in relation to a control group⁽⁶⁾. It also observed that, in the case of unilateral clefts, there is no volumetric difference between the nasal cavities on the sides affected and not affected by the cleft, while other authors have demonstrated that the side affected by the cleft is volumetrically smaller than the unaffected one⁽⁷⁾. However, in 2017, a study involving patients aged between 9 and 12 years with bilateral and unilateral clefts concluded that these patients were not more likely to have nasopharyngeal obstruction compared to their age-matched controls⁽⁸⁾.

Previous studies from our research group have shown, by means of rhinometric and rhinomanometric evaluation, that rapid maxillary expansion, a procedure widely used to correct maxillary transverse deficiency, has been shown to significantly increase the internal nasal dimensions of children with unilateral cleft lip and palate by 26%⁽⁹⁾ and bilateral by 20%⁽¹⁰⁾, improving the nasal patency in these patients.

Thus, it is ideal to evaluate nasal patency because of the importance and need to objectively analyze the results of nasal interventions in individuals with CLP⁽⁴⁾.

Cone-beam computed tomography (CBCT) is considered the gold standard for visualizing the nasal cavity. Several three-dimensional analysis programs have proven capable of reproducing, with high agreement, variables such as the volume, length, and minimum sectional area of the upper airway, and are reliable and accurate tools for three-dimensional analysis of the upper airway^(11,12). CBCT is a type of tomography that provides lower doses of radiation when compared to the conventional one and overcomes the limitations of plain radiography by not having restrictions of cephalometric orientation and noise, among others⁽¹³⁾. Nevertheless, the inadvertent use of this method should be analyzed⁽¹³⁾.

In addition to CBCT, other methods are used for the evaluation of internal nasal dimensions, such as acoustic rhinometry (AR), which allows the identification of nasal cavity constriction sites through consecutive measurements of different cavity segments, ranging from the nostrils to the nasopharynx⁽¹⁴⁾. This method

has the advantage of not being restricted to the measurement of the segment of greatest constriction and does not require patient cooperation, as in the case of rhinomanometry⁽⁴⁾. Thus, the non-invasive technique has shown the importance of using objective methods to follow the development of procedures that have great potential to interfere with the morphophysiology of the nasal cavity, such as rhinoseptoplasty⁽¹⁰⁾.

In this context, the present study aimed to compare the nasal cavity geometry of children and adolescents with CLP and maxillary atresia using CBCT, which is considered the gold standard, and acoustic rhinometry.

METHOD

Participants

The study was approved by the Ethics Committee on Human Research of the Hospital for Rehabilitation of Craniofacial Anomalies of the University of São Paulo, under opinion number 2.190.137.

The study sample consisted of CBCT and AR examinations of 17 individuals with previously repaired complete unilateral CLP and anteroposterior and transverse maxillary atresia, evaluated in a cross-sectional manner, which were previously obtained for orthodontic planning purposes.

As inclusion criteria in the study, we considered examinations of patients from the population of children and adolescents, an adolescent being an individual who is between the ages of ten and 19 years (World Health Organization)⁽¹⁵⁾, with complete unilateral CLP, absence of craniofacial syndromes associated with CLP, and the presence of anteroposterior maxillary deficiency, characterized essentially by the presence of a class III malocclusion.

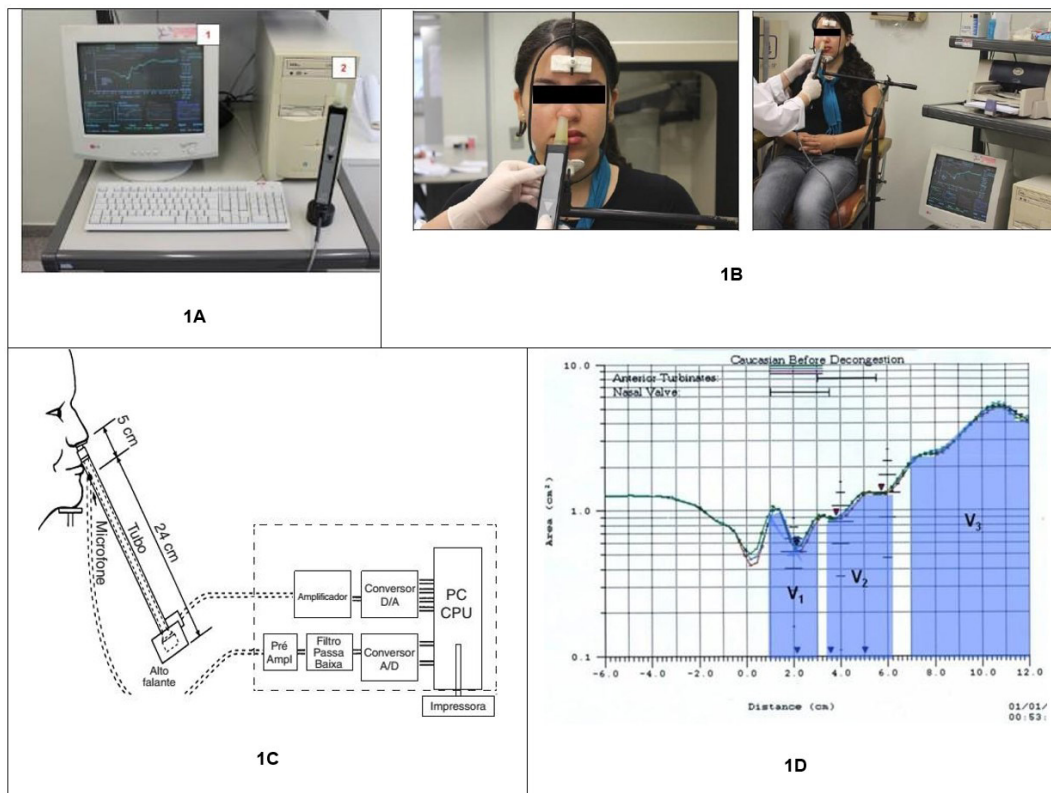
The two examinations were performed on the same day or with only a one-day difference between them, considering the dynamics of the institution and the patients' availability.

Procedures

Acoustic rhinometry (AR)

The volumes provided by the AR technique were calculated in the examinations previously performed routinely for pre-treatment evaluation purposes. The examinations were carried out by two speech and language therapists who were trained and calibrated for the execution of the technique, with 7 and 10 years of experience in the area, respectively, and who work in the clinical routine of the institution where the study was conducted.

The examination uses the Eccovision Acoustic Rhinometer system, which consists of a 24-cm tube, whose distal portion has a sound source (speaker) and the proximal portion a recording microphone (Figure 1A). It is based on the reflection of sound waves that are incident on the nasal cavity and is always performed in the same room, in an environment with relatively stable temperature and humidity (24 °C and approximately 50%, respectively) and with a noise level not exceeding



Legend: 1 = rhinometer 2 = computer monitor showing a rhinogram. View the patient in the position for data acquisition V1: nasal valve region, V2: turbinate region, and V3: nasopharyngeal volume

Figure 1. Acoustic rhinometer (Eccovision, Hood Laboratories): Instrumentation to check transverse areas of the nasal cavity

60 dB, after a period of 30 min for the patient to adapt to the environmental conditions. In this way, we attempted to avoid possible measurement errors due to external noise and variations in ambient temperature.

AR is performed as follows: the tube is held against one nostril, and the sound waves generated in the speaker propagate along the tube and enter the nasal cavity. If there are variations in the cross-sectional area, that is, any constrictions that decrease the lumen of the cavity, the sound waves are reflected as an echo back into the tube. For the best data, the rhinometer is always positioned parallel to the nose dorsum, and a seal is made between the nasal adapter and nasal cavity with a neutral electrocardiogram gel to avoid sound loss (Figure 1B). In addition, to keep the patient's head stable during the examination in a position parallel to the ground, a support is used to support the chin and forehead. The pressure signals of the reflected wave sensitize the microphone, are amplified and digitalized, and then passed to a microcomputer equipped with a specific program for analysis (Figure 1C).

The nasal cross-sectional area and constriction distance are calculated based on the echo intensity and the ratio between the echo velocity and time of arrival, respectively. The data are presented in a graph, the rhinogram, on the computer screen, and in the area-distance function, where the x-axis shows the distance (in cm) and the y-axis is the area on a logarithmic scale (in cm^2) (Figure 1D). Measurements are made in rapid succession, approximately every 0.5 s, throughout the nasal cavity, on the right and left sides, independently⁽¹³⁾. From the

area and distance variables, it is possible to obtain the volume of nasal regions (V1, V2, and V3) provided by the examination itself, corresponding to the region under the rhinogram curve (Figure 1D). For comparison purposes, we considered the total volume of the nasal cavity in the AR, the sum of the values of V1 (volume of the nasal valve region) and V2 (volume of the anterior region of the inferior turbinate) (cm^3), and the value of the region covered by the polygon described in Figure 2, which corresponds to the space of V1 and V2 in the AR.

Cone-beam computed tomography (CBCT)

Cone-beam computed tomography scans were obtained for surgical planning purposes using the i-CAT Next Generation tomograph (ISI- i-CATImaging System - cone beam, Next Generation i-CAT®), and the following specifications were used: a field of view of 16×13 cm, exposure time of 26.9 seconds, 120 Kv, 37.07 mA, and resolution of 0.25. The images were originally generated using .xstd extension and then imported and saved in DICOM extension (Digital Imaging and Communications in Medicine) to be visualized in Dolphin Imaging 11.8 image analysis software.

The images were analyzed by two evaluators who were trained to perform the measurements. The training, which lasted approximately 2 months, consisted of three stages:

- 1) Lecture cycle: lecture 1—principles of tomographic images acquisition (IKTS) / lecture 2—CBCT (IKTS) / lecture 3—tomographic aspects of cleft lip and palate and upper airway (IKTS and SHKT).

- 2) Training in the functionalities of the Dolphin software and use of the available tools for 3D upper airway reconstruction (IKTS).
- 3) Pilot study for reconstruction of the 3D images in 10 images, repeated two times for reproducibility (less experienced evaluator being instructed by the more experienced one).

Evaluator 1 (CAH), a speech and language therapy student; thus, the less experienced evaluator, and Evaluator 2 (IKTS), the research supervisor; thus, the more experienced evaluator, read the images at two different times (T1 and T2), with a two-week interval between measurements, to assess the intra- and inter-evaluator reproducibility. The mean volume values obtained by the two evaluators in the two measurements were considered for the analysis.

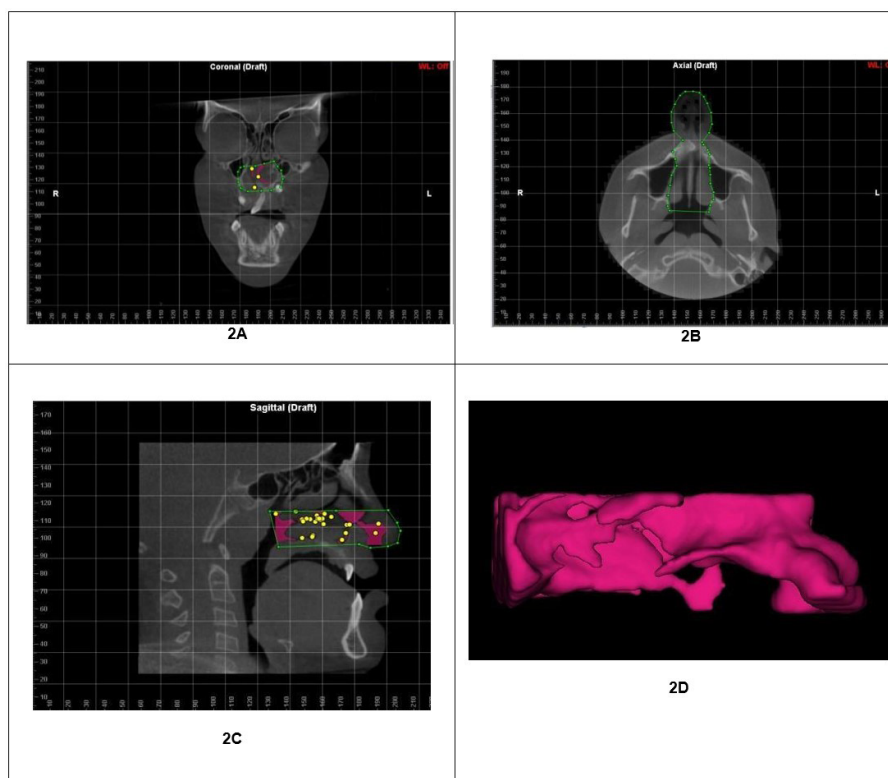
Before delimiting the nasal cavity, the skull of each computed tomography scan was oriented parallel to the ground, according to the temporal bone ostium and the base of the eyeball (Frankfort plane).

The CBCT scans were then evaluated using Dolphin Imaging 11.8 software, which allows the reformatting of the airway image in 3D. The internal volume of the nasal cavity was obtained from the coronal, axial, and sagittal slices of the polygons that delimit the nasal cavity through the following steps:

- 1) On the coronal section, in the anteroposterior direction, the section in which the crista galli appears completely was selected. In this section, the polygon was marked, whose upper limit is constituted by the upper part of

the lower turbinates on both sides, forming an irregular line. The rest of the nasal cavity was contoured, establishing the limit between the nasal cavity and maxillary sinuses, which encompassed the piriform aperture, up to the anterior nasal spine, and closed the polygon. (Figure 2A).

- 2) In the axial section, the section in which the first time the nasal tip appears completely in the inferosuperior direction was selected. In this section, the posterior limit of the polygon is formed by a line parallel to the ground, joining the two ends of the pterygoid processes of the sphenoid bone. Next, the entire nasal cavity was contoured up to the end of the pyriform aperture on both sides. Finally, from the piriform extremities, the contour of the soft tissue of the nose was started, closing the polygon, as illustrated in Figure 2B.
- 3) On the median sagittal section, the polygon by joining the following points was demarcated: N' (Nasal: the most inferior and anterior point between the nasal bones), thereafter, the soft tissue of the nose to point SN (subnasal: the point of intersection between the columella and the labial philtrum) was outlined, ANS (anterior nasal spine: the most anterior point of the intermaxillary suture projection), PNS (posterior nasal spine: the most posterior point of the intermaxillary suture projection), the most posterior point of the inferior turbinate, following to the sphenoid sinus and finally joining the N'. (Figure 2C).
- 4) Once the polygons were delimited, the marking of the nasal airway space contained in these polygons was proceeded with the "seed point" tool, which automatically colored the



Legend: Polygons delineating the nasal cavity in coronal (3A), axial (3B), and sagittal (3C) sections and three-dimensional image of the nasal cavity obtained from the three polygons (3D)

Figure 2. Dolphin Imaging Software: CBCT of nasal cavity

area of interest. Thus, a three-dimensional image of the nasal cavity was generated, and the numerical volume values were calculated and expressed in cm³, as illustrated in Figure 2D.

Thus, in CBCT, the value of the region covered by the polygon described in Figure 2 corresponded, for comparison purposes, to the space of V1 and V2 of the AR.

Data analysis

Considering an alpha error of 5%, a test power of 80%, an expected standard deviation of 1.27⁽¹²⁾, and a minimum difference of 1 cm³, we estimated a minimum sample size of 15 individuals per group.

Intra-evaluator reproducibility was calculated using the intraclass correlation coefficient (ICC)⁽¹⁶⁾, which adopted the following score: ICC < 0.40, weak agreement; ICC of 0.4–0.75, moderate agreement; and ICC > 0.75, high agreement. If the ICC had a high value, the analysis of only 35% of the sample at T2 by Evaluator 2 was considered sufficient for comparative purposes.

Since the volume variable followed a normal distribution, the Kolmogorov Smirnov thesis was used, and the results of the groups were expressed as mean ± standard deviation (X±SD). For comparison of the quantitative variable volume, the significance of the differences between the two tests (AR and CBCT) was assessed by Student's t-test for paired samples. Statistical significance was set at p < 0.05.

RESULTS

The intraclass correlation coefficients in the tomographic evaluation were 0.90 and 0.82, respectively, for intra- and inter-

examiner evaluations. Considering the high rates of agreement, for analysis purposes, the values of Evaluator 1, who completed the analysis of all the samples at both the moments, were presented and analyzed.

Table 1 shows the results of the internal nasal volume measured using acoustic rhinometry and CBCT by Evaluator 1 at the first moment (CBCT_E1_M1) and the second moment (CBCT_E1_M2), as well as the measurements by Evaluator 2 at the two moments (CBCT_E2_M1 and CBCT_E2_M2).

Volume results using AR and CBCT corresponded to 6.6 ± 1.9 cm³ and 8.1 ± 1.5 cm³, respectively. The difference between the examinations was 17.7%, which was considered statistically significant (p = 0.006). Despite the statistical difference observed, Figure 3 shows that, except for patients 4 and 15, who were considered outliers, the volumetric results are equivalent, that is, there is an equivalence between the measurements or, more, a similarity between the curves, or the same pattern.

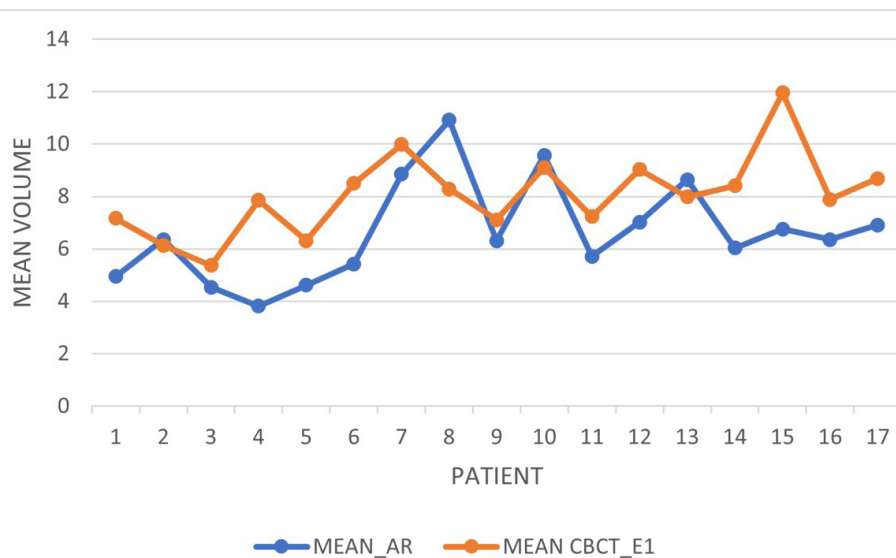
DISCUSSION

Contrary to the initial hypothesis, the results of the present study show that the nasal volumes obtained by AR and CBCT are different. This is probably due to the difficulties encountered in tomographic reconstruction. Although the program used for the tomographic analysis is a good method for the volumetric evaluation of the pharynx⁽¹⁷⁻¹⁹⁾, it proved to be ineffective for the 3D measurement of the nasal cavity. This is because the exclusive delimitation of the nasal cavity, excluding the paranasal sinuses, was always a technical challenge that was difficult to

Table 1. Individual and mean internal nasal volumes measured by acoustic rhinometry (AR) and cone-beam computed tomography (CBCT, in cm³), of evaluators 1 and 2, at moments 1 and 2

PACIENT	MEAN_AR	CBCT_E1_M1	CBCT_E1_M2	MEAN CBCT_E1	CBCT_E2_M1	CBCT_E2_M2	MEAN CBCT_E2
1	4.95	7.61	6.70	7.16	6.54	8.07	7.31
2	6.35	5.76	6.50	6.13	8.48	7.21	7.85
3	4.54	5.45	5.28	5.37	5.85		
4	3.82	7.90	7.80	7.85	7.75		
5	4.61	5.99	6.63	6.31	5.4		
6	5.42	8.58	8.41	8.50	8.23		
7	8.85	10.61	9.35	9.98	10.47		
8	10.91	8.34	8.21	8.28	8.47		
9	6.31	6.94	7.27	7.11	6.56		
10	9.57	8.98	9.21	9.10	8.86		
11	5.71	6.80	7.65	7.23	6.79		
12	7.02	8.87	9.19	9.03	8.38		
13	8.64	7.75	8.23	7.99	8.25	8.15	8.2
14	6.03	8.68	8.14	8.41	6.61		
15	6.76	11.57	12.34	11.96	13.83	12.18	13.01
16	6.36	7.09	8.68	7.89	6.73	9.01	7.87
17	6.91	8.94	8.42	8.68	9.43	9.21	9.32
x	6.6	8.0	8.1	8.1 (17.7%)	8.0	9.0	8.9
sd	1.9	1.6	1.5	1.5	2.0	1.7	2.1
p		0.20				0.09	
		0.006					

Legend: acoustic rhinometry (AR), cone-beam computed tomography (CBCT), evaluator (E), moment (M)



Legend: Acoustic rhinometry (RA), cone-beam computed tomography (TCFC), evaluator (A)

Figure 3. Graph of mean nasal volumes (cm³) measured by acoustic rhinometry and cone-beam computed tomography of the 17 subjects. Values of evaluator 1

overcome, making CBCT volumetric measurements always larger than those of AR.

In this sense, the choice of the polygon format to delimit the nasal cavity in the sagittal plane underwent adjustments throughout the study and was based on the assumption that the volumes of the posterior nasal regions measured by AR were not reliable⁽²⁰⁾, since the sound from the rhinometer, when reaching this region had already suffered many reflections and was dissipated into the pharynx. Thus, we decided to exclude the value of V3 from the volume analyzed, both in the AR and CBCT.

Furthermore, with the tools available in Dolphin Imaging 11.8, as already mentioned, it was not always possible to completely exclude the sinuses adjoining the nasal cavity. It was not uncommon for these structures to be colored and segmented together with the nasal cavity. Thus, based on the premise that CBCT did not reflect the clinical reality, the proposed polygon included the entire nasal base of regions V1 and V2, excluding the region of the middle and upper turbinates. This decision was based on two factors: 1) a study⁽²¹⁾ that proposed a polygon similar to the present study to delimit the nasal cavity, and 2) it was at the nasal base that the acoustic axis of the sound generated by AR was distributed; that is, this was the main path through which the sound waves traveled because of the greater volume of this portion.

In a study⁽²²⁾ comparing nine acoustic rhinometry and computed tomography scans of adult patients with nasal obstruction due to hypertrophic turbinates, the authors analyzed the three minimal sectional areas of the cavity, corresponding to the notches present in the rhinogram, both in AR and CBCT (defined by anatomical landmarks). They observed that areas 1 and 2, corresponding to the first and second notches, had statistically significant correlations between the two methods, while in area 3, which indicated the third notch, in the most posterior region of the nose, no correlation was observed.

Subsequently, in a study of the nasal cavities of six healthy individuals, in which area-distance curves (comparable to the rhinogram) were obtained from both AR and CBCT, a similarity was observed between the curves in the anterior part of the nasal cavity. However, in the posterior region, the results of AR were always higher than those of CBCT, with divergent curves, but with the same pattern. In the epipharynx, measurement errors exceeding 100% were found, even when individualized measurement planes were used, as was the case with the central lines, obtained from the mathematical calculation of the centers of each sectional plane of the cavity. These results indicate that AR has a diagnostic capability for the anterior and not the posterior parts⁽²³⁾.

In 2018, in cases of mouth-breathing patients with transverse maxillary deficiency and posterior crossbite, a comparison was made between the data provided by AR and the widths of different regions of the nasal cavity measured using CBCT. Among the results, the volume provided by rhinometry corresponded only to width 4, which corresponded to the base of the nasal cavity, measured by a horizontal line on the outer border of the palatine region of the maxillary bone, in the coronal plane passing through the most anterior part of the middle turbinate. Other width data corresponded to the superior regions of the nasal cavity⁽²⁴⁾. Thus, it can be said that the nasal volume has a greater anatomical influence from the region below the middle turbinates than from the rest of the cavity, as was observed in the present study.

In 2016, another study⁽²¹⁾ using the same instruments as in the present study (AR and CBCT), as well as the Dolphin Imaging software, also observed that for the total volume of the nasal cavity, CBCT measurements were slightly larger than those of AR. However, the delimited nasal cavity differed from the methodology used in the present study. The two had the upper limit in common as both studies did not cover the uppermost part of the nose. However, as for the posterior part, the study cited

involved the nasopharyngeal region, which was not involved in the present study. The results obtained for the total volumetric mean showed a low correlation with the AR ($r = 0.274$).

This difference in the nose delineation may explain the reason for the low correlation, since the anterior nasal region, measured separately in the 2016 investigation⁽²¹⁾, showed a good correlation ($r = 0.786$), again, corroborating the literature findings cited^(22,23). In addition, another factor that differed from the present study was the individuals who comprised the sample, which in the case of the aforementioned studies were individuals who sought orthodontic treatment and underwent CBCT, but it was not specified if there was a cleft.

While there was no correlation between AR and CBCT, researchers have shown that Dolphin Imaging has a good reliability for oropharyngeal analysis, with a difference of less than 2% compared to a measurement model whose measurements were previously known⁽²⁵⁾. However, their study evaluated pharyngeal volumes and not nasal volumes, which are known to present great technical difficulty for segmentation. Thus, based on this study, the authors asked the following research question: Is rhinometry an effective method for calculating nasal volumes? It is possible that the sound emitted by the equipment is not able to enter all the internal spaces of an obstructed nose, such as those of patients with cleft lip and palate.

On the contrary, the literature⁽²⁵⁾ also describes some disadvantages of the Dolphin Imaging software, such as the lack of tools to segment the desired area more precisely, because its segmentation algorithm still allows some parts to overflow. In the case of the nose, the cavity itself does not have well-established limits because anatomically, its space continues into the maxillary and ethmoidal sinuses. Thus, the segmentation of the desired airway space was impaired several times, involving the sinuses mentioned, and leading the researcher to choose between excluding the part of what is considered the nasal cavity or including the part of other spaces that do not correspond to the nose.

The next step in this study is the tomographic evaluation of the different segments of the nasal cavity, as provided by the AR itself. We speculate that, similar to the aforementioned studies, equivalence in V1 and V2 between the two methods may be found, even in patients with cleft lip and palate, whose anatomy is significantly altered. Additionally, a larger sample evaluating the cavity in its different segments may indicate a similarity between the two methods of analysis.

CONCLUSION

It is concluded that the nasal volumes measured by the two methods, AR and CBCT, are different, presenting discrepancies in the measurements. The gold standard technique (CBCT) identified higher volumes in the nasal cavity than AR.

ACKNOWLEDGEMENTS

To the São Paulo State Research Support Foundation (FAPESP) for funding this study and stimulating, once again, Brazilian Science.

REFERENCES

1. Murray JC. Gene/environment causes of cleft lip and/or palate. *Clin Genet*. 2002;61(4):248-56. <http://dx.doi.org/10.1034/j.1399-0004.2002.610402.x>. PMID:12030886.
2. Freitas JAS, Neves LT, Almeida ALPF, Garib DG, Trindade-Suedam IK, Yaedú RYF, et al. Rehabilitative treatment of cleft lip and palate: experience of the Hospital for Rehabilitation of Craniofacial Anomalies/USP (HRAC/USP) - Part 1: overall aspects. *J Appl Oral Sci*. 2012;20(1):9-15. <http://dx.doi.org/10.1590/S1678-77572012000100003>. PMID:22437671.
3. Bertier CE, Trindade IEK, Silva Filho OG. Cirurgias primárias de lábio e palato. In: Trindade IE, Silva Filho OG. *Fissuras labiopalatinas: uma abordagem Interdisciplinar*. São Paulo: Ed. Santos; 2007. p. 73-86.
4. Bertier CE, Trindade IEK. Deformidades nasais: avaliação e tratamento cirúrgico. In: Trindade IE, Silva Filho OG. *Fissuras labiopalatinas: uma abordagem Interdisciplinar*. São Paulo: Ed. Santos; 2007. p. 87-107.
5. Freitas JAS, Trindade-Suedam IK, Garib DG, Neves LT, Almeida ALPF, Yaedú RYF, et al. Rehabilitative treatment of cleft lip and palate: experience of the Hospital for Rehabilitation of Craniofacial Anomalies/USP (HRAC/USP) - Part 5: Institutional outcomes assessment and the role of the Laboratory of Physiology. *J Appl Oral Sci*. 2013;21(4):383-90. <http://dx.doi.org/10.1590/1678-775720130290>. PMID:24037080.
6. Farzal Z, Walsh J, Lopes de Rezende Barbosa G, Zdanski CJ, Davis SD, Superfine R, et al. Volumetric nasal cavity analysis in children with unilateral and bilateral cleft lip and palate. *Laryngoscope*. 2016;126(6):1475-80. <http://dx.doi.org/10.1002/lary.25543>. PMID:26267849.
7. Starbuck JM, Friel MT, Ghoneima A, Flores RL, Tholpady S, Kula K. Nasal airway and septal variation in unilateral and bilateral cleft lip and palate. *Clin Anat*. 2014;27(7):999-1008. <http://dx.doi.org/10.1002/ca.22428>. PMID:24976342.
8. Al-Fahdawi MA, Farid MM, El-Fotouh MA, El-Kassaby MA. Cone-beam computed tomography analysis of the nasopharyngeal airway in nonsyndromic cleft lip and palate subjects. *Cleft Palate Craniofac J*. 2017;54(2):202-9. <http://dx.doi.org/10.1597/15-134>. PMID:26752132.
9. Trindade IE, Castilho RL, Sampaio-Teixeira AC, Trindade-Suedam IK, Silva Filho OG. Effects of orthopedic rapid maxillary expansion on internal nasal dimensions in children with cleft lip and palate assessed by acoustic rhinometry. *J Craniofac Surg*. 2010;21(2):306-11. <http://dx.doi.org/10.1097/SCS.0b013e3181cf5f5f>. PMID:20186095.
10. Trindade-Suedam IK, Castilho RL, Sampaio-Teixeira AC, Araújo BM, Fukushiro AP, Campos LD, et al. Rapid maxillary expansion increases internal nasal dimensions of children with bilateral cleft lip and palate. *Cleft Palate Craniofac J*. 2016;53(3):272-7. <http://dx.doi.org/10.1597/14-244>. PMID:25591126.
11. Chen H, van Eijnatten M, Wolff J, de Lange J, van der Stelt PF, Lobbezoo F, et al. Reliability and accuracy of three imaging software packages used for 3D analysis of the upper airway on cone beam computed tomography images. *Dentomaxillofac Radiol*. 2017;46(6):20170043. <http://dx.doi.org/10.1259/dmfr.20170043>. PMID:28467118.
12. Guijarro-Martínez R, Swennen GRJ. Cone-beam computerized tomography imaging and analysis of the upper airway: a systematic review of the literature. *Int J Oral Maxillofac Surg*. 2011;40(11):1227-37. <http://dx.doi.org/10.1016/j.ijom.2011.06.017>. PMID:21764260.
13. Ludlow JB, Davies-Ludlow LE, Brooks SL, Howerton B. Dosimetry of 3 CBCT devices for oral and maxillofacial radiology: CB Mercuray, NewTom 3G and i-CAT. *Dentomaxillofac Radiol*. 2006;35(4):219-26. <http://dx.doi.org/10.1259/dmfr/14340323>. PMID:16798915.
14. Hilberg O, Pedersen OF. Acoustic rhinometry: recommendations for technical specifications and standard operating procedures. *Rhinol Suppl*. 2000;16:3-17. PMID:11225287.
15. WHO: World Health Organization. Regional Working Group on Health Needs of Adolescents: Final Report. WHO Document ICP/MCH/005. Manila: World Organization, Regional Office for the Western Pacific; 1980.
16. Fleiss J. The design and analysis of clinical experiments. New York: Wiley; 1986.

17. Trindade-Suedam IK, Lima TF, Campos LD, Yaedú RY, Filho HN, Trindade IEK. Tomographic pharyngeal dimensions in individuals with unilateral cleft lip/palate and Class III malocclusion are reduced when compared with controls. *Cleft Palate Craniofac J*. 2017;54(5):502-8. <http://dx.doi.org/10.1597/15-124>. PMID:27148639.
18. Pinheiro ML, Yatabe M, Ioshida M, Orlandi L, Dumast P, Trindade-Suedam IK. Volumetric reconstruction and determination of minimum cross-sectional area of the pharynx in patients with cleft lip and palate: comparison between two different softwares. *J Appl Oral Sci*. 2018;26(0):e20170282. <http://dx.doi.org/10.1590/1678-7757-2017-0282>. PMID:30304121.
19. Yatabe-Ioshida MS, Campos LD, Yaedú RY, Trindade-Suedam IK. Upper Airway 3D Changes of patients with cleft lip and palate after orthognathic surgery. *Cleft Palate Craniofac J*. 2019;56(3):314-20. <http://dx.doi.org/10.1177/1055665618778622>. PMID:29846086.
20. Cakmak O, Tarhan E, Coskun M, Cankurtaran M, Çelik H. Acoustic rhinometry: accuracy and ability to detect changes in passage area at different locations in the nasal cavity. *Ann Otol Rhinol Laryngol*. 2005;114(12):949-57. <http://dx.doi.org/10.1177/000348940511401211>. PMID:16425563.
21. Tsolakis IA, Venkat D, Hans MG, Alonso A, Palomo JM. When static meets dynamic: comparing cone-beam computed tomography and acoustic reflection for upper airway analysis. *Am J Orthod Dentofacial Orthop*. 2016;150(4):643-50. <http://dx.doi.org/10.1016/j.ajodo.2016.03.024>. PMID:27692422.
22. Gilain L, Coste A, Ricolfi F, Dahan E, Marliac D, Peynegre R, et al. Nasal cavity geometry measured by acoustic rhinometry and computed tomography. *Arch Otolaryngol Head Neck Surg*. 1997;123(4):401-5. <http://dx.doi.org/10.1001/archotol.1997.01900040037006>. PMID:9109788.
23. Terheyden H, Maune S, Mertens J, Hilberg O. Acoustic rhinometry: Validation by Three-Dimensionally Reconstructed Computer Tomographic Scans. *J Appl Physiol*. 2000;89(3):1013-21. <http://dx.doi.org/10.1152/jappl.2000.89.3.1013>. PMID:10956345.
24. Sakai RHUS, Marson FAL, Sakamura ETI, Ribeiro JD, Sakano E. Correlation between acoustic rhinometry, computed rhinomanometry and cone-beam computed tomography in mouth breathers with transverse maxillary deficiency. *Rev Bras Otorrinolaringol (Engl Ed)*. 2018;84(1):40-50. <http://dx.doi.org/10.1016/j.bjorl.2016.10.015>.
25. Weissheimer A, Menezes LM, Sameshima GT, Enciso R, Pham J, Grauer D. Imaging software accuracy for 3-dimensional analysis of the upper airway. *Am J Orthod Dentofacial Orthop*. 2012;142(6):801-13. <http://dx.doi.org/10.1016/j.ajodo.2012.07.015>. PMID:23195366.

Authors' contribution

CAH was one of the evaluators responsible for measuring the airways, as described in the article's methodology, and contributed to the formatting and part of the writing of the manuscript; MAGU was responsible for performing part of the measurements, contributing as another evaluator and assisting in statistics and procedures; MSYI performed the step to obtain measurements by acoustic rhinometry; IEKT contributed to the article's methodological definition, helping to define reference points for performing the tomographic measurements; APF assisted in article writing and formatting; DGGC was responsible for carrying out the procedures to obtain the orthodontic examinations used in the research; and IKTS guided the entire research from its conception to completion, making the decision to submit the article for publication in this journal and contributing to its writing.